Hot electron injection driven phase transitions

Masaki Hada, Dongfang Zhang, Albert Casandruc, and R. J. Dwayne Miller*
Max Planck Research Department for Structural Dynamics, Center for Free Electron Laser Science, University of Hamburg, c/o DESY, Notkestrasse 85, Hamburg 22607, Germany

Yusaku Hontani and Jiro Matsuo
Quantum Science and Engineering Center, Kyoto University, Gokasho, Uji, Kyoto 611-0011, Japan

Robert E. Marvel and Richard F. Haglund Jr.
Department of Physics and Astronomy, Vanderbilt University, 6301 Stevenson Center, Nashville, Tennessee 37235, USA
(Received 17 July 2012; revised manuscript received 5 September 2012; published 1 October 2012)

We report on a general mechanism for photo-induced phase transitions. The process relies on the photo-injection of hot electrons from an adjacent metallic layer to trigger the structural dynamics of the materials of interest. This mechanism is demonstrated for the semiconductor-to-metal phase transition of VO_2 using a 20 nm Au injection layer. The nature of the phase transition is demonstrated by time-resolved optical transmission measurements, as well as a well defined bias dependence that illustrates that the Au film is the source of nonequilibrium electrons driving the phase transition.

DOI: 10.1103/PhysRevB.86.134101 PACS number(s): 73.40.−c, 68.35.−p, 78.47.J−

I. INTRODUCTION

Photo-induced ultrafast electronic excitations cause a variety of unconventional phenomena such as nonthermal melting,[1] bond-hardening effects,[2] vapor condensation,[3] semiconductor-to-metal phase transitions (SMTs),[4–6] and enhancement of superconductivity.[7,8] The photo-induced phenomena associated with strongly correlated electron materials[9,10] have generated intense interest due to the relatively large change in material properties that can be optically gated. This interest is driving the synthesis and characterization of new materials that exhibit complex behavior.

The SMT in transition-metal oxides is a canonical example of these strongly correlated systems. SMT occurs in thermal cycling[11] i.e., the transition metal oxide is usually stable in the metallic phase at temperatures higher than a critical temperature (T_c). Frequently, the lattice and electronic structures are governed by Peierls lattice instabilities or Mott charge localization reducing charge migration and conferring semiconductor properties when the temperature is lowered or raised. Ultrafast optical excitation has been used to control the phase of these materials. The photo-excited electron-hole pairs drive the lattice modification and simultaneously induce a profound change in their electrical properties. This phenomenon has been extremely well characterized for vanadium dioxide (VO_2), in large measure due to interest in this material as a nonlinear optical limiter.

Using this system, we demonstrate a new mechanism for inducing structural phase transitions that promises to be fully general, i.e., independent of material optical properties, by using a secondary source to photo-inject nonequilibrium electrons to alter the lattice potential. In this respect, we characterized the SMT in Au-coated VO_2 with femtosecond pump-probe transmission experiments in which the Au layer serves as a photo-injector of hot electrons into the adjacent VO_2 layer. In this series of experiments, the optical excitation pulses are absorbed almost entirely within the Au layer. The optical transmission into the VO_2 layer is too small to optically induce the SMT directly in the underlying VO_2 substrate; however, its ultrafast SMT was still observed. Through a number of control studies, the ultrafast induced phase transition was shown to be unique to the VO_2/Au contact.

The key experiment was a bias dependence that demonstrated that the correlation of the optically induced phase transition was attributable to photo-induced nonequilibrium electrons originating in the Au layer as opposed to thermal transport. In this scenario, the phase transition arises from the hot electrons from the Au contact layer that serves as the photo-injector to create conditions of nonequilibrium electrons into the conduction band of the adjacent layer. The antibonding nature of these electronic states destabilizes the lattice potential that is unique to conditions of excess electron occupation in the conduction band states, which, above a critical density, leads to lattice instability and ensuing structural transition. This mechanism could be particularly important as a general optical trigger of critical phenomena to fully exploit the recent advances in ultrabright x-ray and electron sources for atomically resolved structural dynamics. This mechanism can be applied to a wide range of strongly correlated materials and is likely applicable in general as long as a metal contact can be made to the material of interest.

The first-order SMT in VO_2 occurs at a T_c of about 340 K[11] and has been discussed as the basis for potential applications ranging from photoactive filters to ultrafast optical switching.[12] The SMT in VO_2 is manifested by large changes in resistivity and dielectric functions[4,13–15] that are accompanied by a simultaneous structural change[16–19] from the low-temperature monoclinic insulating phase with band gap of ∼0.7 eV[20] to the high-temperature rutile metallic phase. It is generally agreed that the SMT arises from a combination of Peierls and Mott mechanisms.[21,22] With respect to the prospect of electron injection, it was reported that there is a charge-transfer effect between either TiO_2 or VO_2 and a Au interface,[23] and the SMT switching effect for VO_2 using this charge transfer approach occurs on the microsecond time

 ©2012 American Physical Society

scale.[24] It has also been observed that the SMT can be assisted by scattering due to the surface plasmon resonance in a nanocomposite comprising an array of Au nanoparticles or thin Au film (∼5 nm) covered by a thin film of VO_2.[25–27] In these cases, where a very thin Au layer was used, the main driving force for the phase transition was the optical photons that passed through the thin Au layer and were absorbed directly into the VO_2 layer. For a thick Au layer (∼20 nm) on top of VO_2 as in the present case, this contribution is avoided by the high absorption of the thicker Au layer. This makes it possible to observe the effect of the injected hot electrons from the optically excited Au on the SMT phase transition of VO_2, without direct excitation of VO_2.

II. EXPERIMENTAL SETUP

A polycrystalline 30 ± 1 nm thick VO_2 layer was grown on a sapphire window or ITO substrate by electron beam evaporation. Some of these samples were subsequently coated with Au films (20 ± 1 nm thickness) by thermal evaporation. VO_2/sapphire, Au/sapphire, Au/VO_2/sapphire, and Au/VO_2/ITO multilayer samples were characterized in conventional optical pump-probe experiments in transmission mode with a 1-kHz regenerative femtosecond laser system that provided excitation wavelengths at 800 nm (pulse duration: ∼40 fs) and probe wavelengths at 400 nm (pulse duration: ∼70 fs). The 800-nm optical pump beam was focused on the sample at an incident angle of 4° with respect to the surface normal, and the 400-nm probe pulse was focused on the excited spot at an incident angle of 30° from the surface normal. The transmission of the samples was detected using standard lock-in methods with a 500 Hz optical chopper. During the optical pump-probe experiments, a variable bias was introduced for the Au/VO_2/ITO multilayer sample (Fig. 1) as a control to determine if the effect arose from ballistic electron transport, as opposed to thermal transport effects that would not be bias dependent. The optical reflectivity, transmission and absorption in each sample were measured: the reflectivity and transmission from the each sample were VO_2/sapphire (28%/57%), Au/sapphire (78%/17%), Au/VO_2/sapphire (76%/18%), and Au/VO_2/ITO (75%/16%). Therefore, the absorption of the incident intensity of each sample can be calculated to be VO_2/sapphire (15%/0%), Au/sapphire (5%/0%), Au/VO_2/sapphire (4%–5%/1%–2%/0%), and Au/VO_2/ITO (4%–5%/1%–2%/3%), respectively. The complex refractive index of Au is $0.18–5.11i$ at a wavelegth of 800 nm. This Au

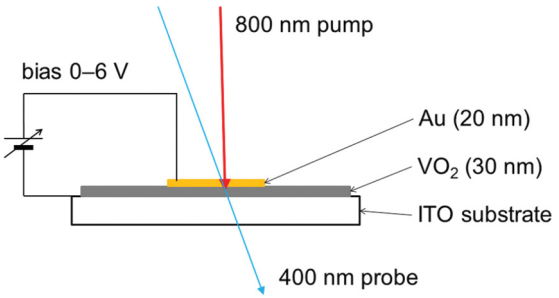

FIG. 1. (Color online) The structure of the Au/VO_2/ITO sample with pump-probe beam geometries and bias direction.

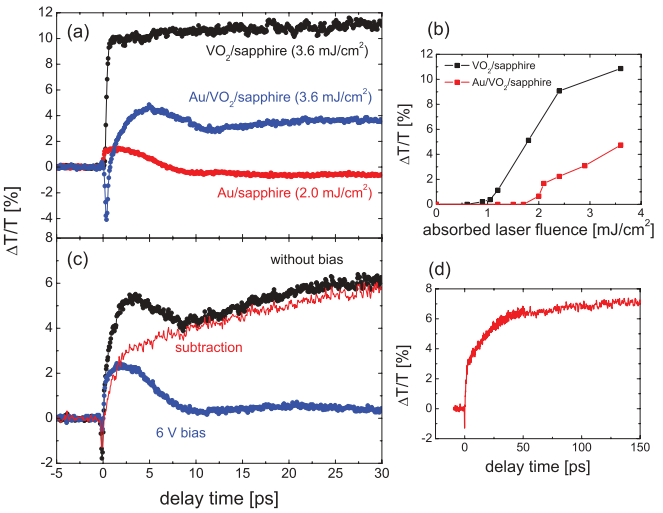

FIG. 2. (Color online) (a) Changes in differential transmission with delay time for VO_2/sapphire, Au/sapphire, and Au/VO_2/sapphire. The legends are inserted in the figure. (b) The threshold of laser-absorbed fluence of the phase transition on VO_2/sappphire and Au/VO_2/sapphire. (c) Changes in transmission as a function of delay time for Au/VO_2/ITO with bias assistance. The red solid lines represent the subtracted change in the transmission of Au/VO_2/ITO with the bias voltage of 6 V from that without bias. (d) The subtracted change with longer delay time.

film was made by the thermal evaporation and the surface of the material is not perfectly flat; therefore, the real part of the refractive index of the Au layer would be 0.2–1. According to Snell's law, the optical penetration depth in the Au film with an incident angle of 4° would be longer than the film thickness (20 nm).

The changes in transmission ($\Delta T/T$) as a function of time for VO_2/sapphire, Au/sapphire, and Au/VO_2/sapphire are shown in Fig. 2(a). The typical photo-induced phase transition was observed in the time-resolved transmission for the VO_2/sapphire sample. The transmission of the VO_2/sapphire sample increased by about 10% with a time constant of ∼100 fs, consistent with previous reports.[6] As shown in Fig. 2(b), the threshold of the absorbed laser fluence for the SMT of this sample was determined to be ∼1 mJ/cm^2 (incident fluence ∼7 mJ/cm^2), which also agrees with previous reports.[13,14,16–18] This excitation level is equivalent to 4×10^{15} photons/cm^2. The excited VO_2 volume (1 cm^2 × 30 nm) contains 9.4×10^{16} valence band electrons. Thus, the optically driven phase transition occurs when about 4% of valence-band electrons are excited to the conduction band. From the changes in transmission as a function of time delay for Au/sapphire, a fast increase (300 fs) and slow relaxation (5 ps) were observed. This change in transient transmission was attributed to hot electron excitation in the Au layer[28,29] that reaches an elevated electronic temperature within 300 fs to slowly equilibrate with the Au lattice through electron-phonon relaxation processes. The thermalization process in Au is slower than in other metals due to the relatively small electron-phonon coupling constants for Au.

Above the absorbed laser fluence of ∼2 mJ/cm^2, the time-resolved transmission in Au/VO_2/sapphire showed the same contributions as that of the directly photo-induced SMT

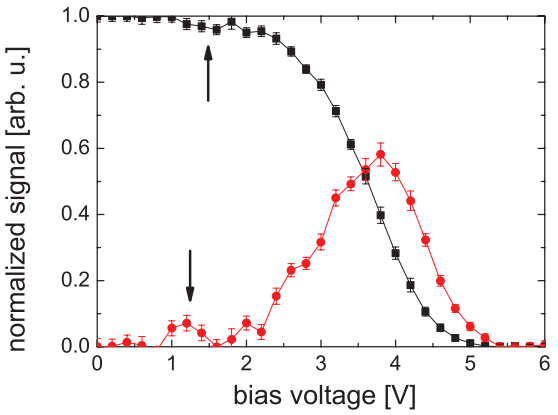

FIG. 3. (Color online) The normalized SMT signal ($\Delta T/T$) at the delay time of ~100 ps as a function of bias voltage. The difference signal with and without bias at 100 ps was normalized to the difference signal without an applied bias and scanned out to 6 V bias. The red curve shows the derivative of this response to highlight the minimum observed at 1.5 V (indicated by the upper arrow) and the inflection point for maximally reducing the electron distribution in the VO_2 half space.

in VO_2. The reduction in the time-resolved transmission of Au/VO_2/sapphire in 300 fs results from excitation of the bulk plasmon in the Au layer. The broad oscillation around 10 ps is attributable to acoustic strain in the Au film. The corresponding phonon frequency for this mode can be calculated by the following equation:[30]

$$f_n = \frac{nv}{2d}, \tag{1}$$

where v is the speed of sound and d is the film thickness. The speed of sound in Au is 3240 m/s and the thickness of the Au film is 20 nm; therefore, the frequency of the acoustic oscillation is calculated to be 81 GHz (period: 12 ps). This value corresponds to the period of the oscillation in Figs. 2(a) and 2(c). It is important to note that, due to the attenuation of the optical excitation by the Au film, this level of excitation is more than four times less than that needed to observe the direct photo-induced SMT of VO_2.

In the key control experiment, a variable bias was applied to the Au/VO_2/ITO structure to affect the spatial distribution of both equilibrium and nonequilibrium electrons. Figure 2(c) shows the time-resolved transmission from the Au/VO_2/ITO multilayer samples with or without bias at an absorbed laser fluence of 3.2 mJ/cm^2. The appearance of the time-resolved transmission from Au/VO_2/ITO without bias is similar to that from Au/VO_2/sapphire. With increasing the bias, i.e., as the hot electrons generated in the Au layer were more confined to the Au half space, the contribution of the SMT in VO_2 to the time-resolved transmission was reduced. The phase transition in VO_2 was completely inhibited with a bias voltage of 5 V. Taking the derivative of the bias dependence, we observed a threshold effect at approximately 3 V, which is direcly related to the electronic temperature of the hot electron disctribution excited in the Au layer. A small drop at approximately 1.3–1.5 V is also observed in the figure, which corresponds to the band gap of the VO_2 (0.7 eV). This point is indicated in Fig. 3 and can be seen by eye as a small minimum in the bias dependence.

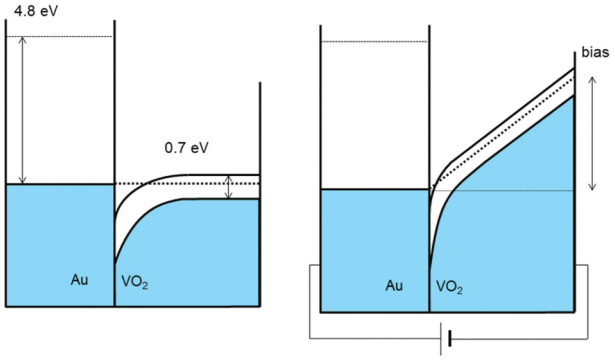

FIG. 4. (Color online) The electron band diagram of Au/VO_2 for ohmic contact. The spatial distribution of the generated hot electrons penetrating into VO_2 will be affected by the potential barrier created by the applied bias.

The time-resolved transmission manifests several complex effects from photo-electron coupling, electron diffusion, ionic motion, and phonon excitation. The applied bias voltage modifies the spatial distribution of the hot electrons within the VO_2 layer, as illustrated in Fig. 4, and isolates the effects of the hot electron distribution on the ensuing dynamics. Other possible explanation, such as thermal transport will be unaffected by an applied bias. Thus, the subtraction of time-resolved transmission from Au/VO_2/ITO with the bias voltage of 6 V from that without bias provides us the changes in transmission invoked solely by transport of electrons into the VO_2 layer. From the subtracted spectra shown in Figs. 2(c) and 2(d), the phase transition in Au/VO_2 and associated change in reflectivity or transmission involves two distinct temporal components: a fast nonthermal component of 2 ps and a slower thermal relaxation component of 40–50 ps, respectively.

III. RESULTS AND DISCUSSIONS

It could be argued that the phase transition is driven by thermally driven stresses, corresponding to an increase in pressure in the phase diagram. This mechanism would develop at the speed of sound. Not taking into account the acoustic propagation across the Au layer, the speed of sound in VO_2 is ~4000 m/s,[31] such that an acoustic stress wave would require about 10 ps to propagate across the VO_2 layer using Eq. (1). Further, the relaxation of the hot electrons into this very acoustic mode takes place on a 5-ps time scale as directly determined above. This mechanism is too slow to explain the fast component (2 ps) observed in the SMT response. The slow SMT component observed in Au/VO_2 samples, however, is fully consistent with a thermal contribution to the signal. The hot electrons generated within the Au layer relax into lattice phonons to increase the effective lattice temperature. Similarly, any hot electrons injected into the VO_2 will subsequently relax into lattice phonons in the VO_2 half space. The thermal profile across this interface will depend on the fraction of hot electrons transferred to the VO_2. This difference in lattice temperature provides the fraction of hot electrons transferred to the VO_2. The associated difference in lattice temperature reflects the gradient for thermal diffusion from the Au into the VO_2 layer. Based on the thermal diffusivity of Au, the observed time

scale of the slow component is consistent with a thermal diffusion contribution from the Au to the VO_2 layer. This clear separation in time scales enables a determination of the purely electronic and thermal or nuclear rms motions on the lattice dynamics that is not readily separable from observation of direct photo-induced effects.

It is interesting to note that the hot-electron-induced phase transition is significantly slower than the direct photo-excitation process, which is well reproduced in the VO_2/sapphire control experiment. The excitation pulses produce a significant number of hot electrons in the Au layer, which are subsequently transported into the underlying VO_2 to induce the SMT. The energy of the hot electrons capable of inducing the SMT in VO_2 can be inferred from the time-resolved transmission measurements with varying bias voltages. As mentioned above, there appears to be a small drop at the bias of about 1.3–1.5 V, which is related to the band gap of VO_2 in the semiconductor phase (0.7 eV). The hot electron distribution in the VO_2 layer will be attenuated by the applied bias. However, when the potential barrier is not higher than the energy of the hot electrons, these nonequilibrium electrons will freely propagate into the VO_2 layer, based on the known band junctions as shown in Fig. 4. To quantify this effect, the normalized phase transition in VO_2 shows an inflection point at 2 V and a half maximum value at approximately 3 V.

To illustrate the effect of the bias on the electron distribution, Fig. 4 shows the electron band diagram with and without bias. Since the Au and VO_2 interface makes an ohmic contact, the bias voltage increases uniformly in VO_2.[23] The hot electrons generated within the Au layer will experience transport conditions under the influence of the initial excess spatial distribution within the Au layer and the triangle potential produced by the bias within the VO_2 region. We can use the observed bias dependence to estimate the number of injected electrons needed to induce the phase transition. The energy of the hot electrons is assumed to be half the bias voltage (~1.5 eV) where appreciable attenuation of the SMT is observed. This phase transition process would be governed by ballistic electron transport. Nevertheless, the temperature of the hot electrons (T_e) produced in the Au layer can be roughly estimated from the absorbed laser fluence (P) and electron heat capacity ($C_s = 67.6\ \mathrm{J\ K^{-2}m^{-3}}$) as[32]

$$P = \int_{T_0}^{T_e} C_s t\, dt = \frac{1}{2} C_s \left(T_e^2 - T_0^2\right), \tag{2}$$

where T_0 is room temperature (293 K). The hot electrons generated in the Au layer would be transported ballistically through the 20-nm layer within 100 fs. According to Eq. (2), the temperature of the hot electrons at the threshold absorbed laser fluence of 2 $\mathrm{mJ/cm^2}$ would be 5500 K (0.5 eV). The density of the hot electrons with the energy of 1.5 eV or greater in the excited Au film is 4.7×10^{15} $\mathrm{electrons/cm^2}$ (4% of the valence band electrons in the Au layer) derived from the Fermi-Dirac distribution. This number of excited, nonequilibrium electrons corresponds to the case of the photo-induced SMT in VO_2. Considering the fact that the penetration depth of the 1.5 eV electrons in VO_2 is a few nanometers, the hot electrons generated in the Au layer and injected into the VO_2 layer would induce the SMT in VO_2 through the direct injection and primary scattering processes to give a nonequilibrium distribution within the VO_2. This change in electron distribution is sufficient to change the lattice stability point to favor the metallic phase.

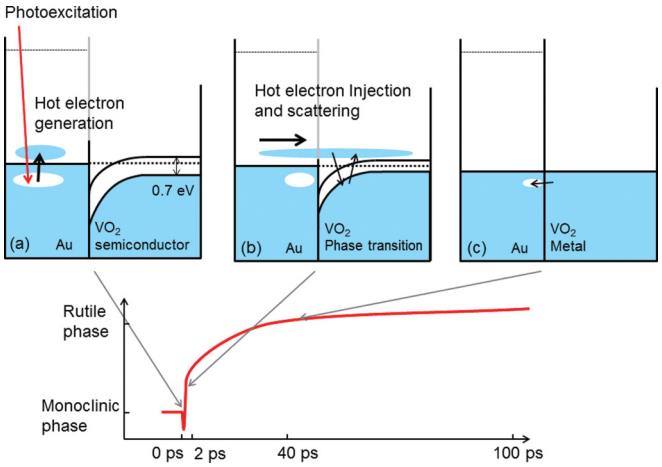

FIG. 5. (Color online) (a) Schematic band diagram of Au/VO_2; (b) the hot electron injection from Au layer to VO_2 layer which leads to the SMT in VO_2; (c) the hot electron recombination with the hole carriers across the interface completes the equilibration of electron distribution, trapping the system in the metallic phase until thermal relaxation over the barrier between the two phases completes the relaxation process. The figure below indicates the time scale of the of the phase transition.

Finally, it is interesting to speculate on the coupled dynamics between the Au and VO_2 layers during the phase transition. There are two equivalent interpretations for the production of nonequilibrium electrons within the VO_2 that lead to this SMT phenomenon. One scenario is that the excited electrons generated in the upper Au layer undergo ballistic transport to the VO_2 layer. The speed of the ballistic electron is around 10^6 m/s,[29] and they would pass through Au (20 nm thickness) and VO_2 (30 nm thickness) layers in around 100 fs. These energetic electrons contribute both nonthermally and thermally through subsequent relaxation processes to the triggered phase transition in VO_2 in a few picoseconds, with the nonthermal contribution dominating on this time scale.

The other scenario is that nonequilibrium electrons undergo transport through the contact between the Au and VO_2. The contact between Au and VO_2 (semiconductor phase) is Ohmic. The exact scenario for nonequilibrium transport between Au and VO_2 does not change the picture for the driving force for the observed SMT. The optical pulse generated hot electrons in the Au layer whose energy distribution is sufficiently below the work function of Au not to escape to the vacuum, but was nevertheless sufficiently high for the electron to tunnel into the conduction band of VO_2 [Fig. 5(a)]. Through the direct injection (non-thermal effect) and primary scattering (thermal effect), the injected hot electrons will transfer the energy to the cold VO_2 lattice, which could trigger the SMT in 2 ps [Fig. 5(b)]. Accompanying the SMT is the evolution of an overlap between the conduction and valence bands.[6] The VO_2 phase transition to the metallic phase involves band-

gap collapse [Fig. 5(c)]. Subsequently, the doped electrons can recombine with the holes at the interface of the Au and metallic VO_2 to trap the system in this metastable phase. It will be interesting to extend the time base to observe the full recovery of the system back to the semiconducting phase. There is apparently a barrier to subsequent relaxation that traps the system for time scales in excess of the 1-ns dynamic range of the present experiment. It should also be noted that, with full thermal equilibrium between the Au and VO_2 half spaces, the lattice temperature is above the phase transition temperature of VO_2 such that the subsequent relaxation back to the semiconducting phase will be dictated by thermal cooling of the structure.

IV. CONCLUSIONS

In conclusion, the ultrafast SMT in Au/VO_2 was investigated in conventional optical pump-probe experiments with the assistance of an applied bias to separate nonthermal electronic and thermal effects. Hot electrons generated in the upper Au layer with 800-nm optical pulses penetrate into the underlying VO_2 layer. The hot electrons couple with the cold lattice in VO_2 immediately upon ballistic transport across the interface and trigger the SMT in VO_2 on the timescale of 2 ps. This result suggests that hot electrons have the potential to induce structural changes in a number of materials that undergo SMT. As a further application, it is interesting to note that, with thermal- or voltage-assisted hot electron excitation, it is possible to achieve ultrafast phase transitions in transparent materials that cannot be excited by optical pulses. This new trigger for inducing structural transitions will extend the number of systems available for atomically resolved dynamics in coming to an atomic level understanding of structural dynamics and connection to electron correlation effects in the ensuing lattice dynamics.[33]

ACKNOWLEDGMENTS

This work was funded by the Max Planck Society through institutional support for the Max Planck Research Group for Structural Dynamics at the University of Hamburg. The Vanderbilt researchers (R.E.M., R.F.H.) acknowledge support of the Office of Science, US Department of Energy (DE-FG02-01ER45916). The authors would like to acknowledge the discussions with T. Seki at Kyoto University and G. Sciaini at the Max Planck Research Department of Structural Dynamics at the University of Hamburg.

*dwayne.miller@mpsd.cfel.de

[1] G. Sciaini, M. Harb, S. G. Kruglik, T. Payer, C. T. Hebeisen, F.-J. Meyer zu Heringdorf, M. Yamaguchi, M. Horn-von Hoegen, R. Ernstorfer, R. J. D. Miller, Nature (London) **458**, 56 (2009).

[2] R. Ernstorfer, M. Harb, C. T. Hebeisen, G. Sciaini, T. Dartigalongue, and R. J. D. Miller, Science **323**, 1033 (2009).

[3] P. Rohwetter, J. Kasparian, K. Stelmaszczyk, Z. Hao, S. Henin, N. Lascoux, W. M. Nakaema, Y. Petit, M. Queisser, R. Salame, E. Salmon, L. Woeste, and J.-P. Wolf, Nat. Photon. **4**, 451 (2010).

[4] M. F. Becker, A. B. Buckman, and R. M. Walser, Appl. Phys. Lett. **65**, 1507 (1994).

[5] S. Iwai, M. Ono, A. Maeda, H. Matsuzaki, H. Kishida, H. Okamoto, and Y. Tokura, Phys. Rev. Lett. **91**, 057401 (2003).

[6] D. Polli, M. Rini, S. Wall, R. W. Schoenlein, Y. Tomioka, Y. Tokura, G. Cerullo, and A. Cavalleri, Nat. Mater. **6**, 643 (2007).

[7] D. Lederman, E. Osquiguil, G. Nieva, J. Guimpel, J. Hasen, Y. Bruynseraede, and I. K. Schuller, J. Supercond. **7**, 127 (1994).

[8] D. Fausti, R. I. Tobey, N. Dean, S. Kaiser, A. Dienst, M. C. Hoffmann, S. Pyon, T. Takayama, H. Takagi, and A. Cavalleri, Science **331**, 189 (2011).

[9] M. Imada, A. Fujimori, and Y. Tokura, Rev. Mod. Phys. **70**, 1039 (1998).

[10] M. Eichberger, H. Schaefer, M. Krumova, M. Beyer, J. Demsar, H. Berger, G. Moriena, G. Sciaini, and R. J. D. Miller, Nature (London) **468**, 799 (2010).

[11] F. J. Morin, Phys. Rev. Lett. **3**, 34 (1959).

[12] H. Coy, R. Cabrera, N. Sepulveda, and F. E. Fernandez, J. Appl. Phys. **108**, 113115 (2010).

[13] A. Cavalleri, M. Rini, and R. W. Schoenlein, J. Phys. Soc. Jpn. **75**, 011004 (2006).

[14] T. L. Cocker, L. V. Titova, S. Fourmaux, G. Holloway, H.-C. Bandulet, D. Brassard, J.-C. Kieffer, M. A. El Khakani, F. A. Hegmann, Phys. Rev. B **85**, 155120 (2012).

[15] S. Wall, D. Wegkamp, L. Foglia, K. Appavoo, J. Nag, R. F. Haglund Jr, J. Staehler, M. Wolf, Nat. Commun. **3**, 721 (2012).

[16] A. Cavalleri, Cs. Toth, C. W. Siders, and J. A. Squier, F. Raksi, P. Forget, and J. C. Kieffer, Phys. Rev. Lett. **87**, 237401 (2001).

[17] P. Baum, D.-S. Yang, A. H. Zewail, Science **318**, 788 (2007).

[18] M. Hada, K. Okimura, and J. Matsuo, Phys. Rev. B **82**, 153401 (2010).

[19] M. Hada, K. Okimura, and J. Matsuo, Appl. Phys. Lett. **99**, 051903 (2011).

[20] S. Biermann, A. Poteryaev, A. I. Lichtenstein, and A. Georges, Phys. Rev. Lett. **94**, 026404 (2005).

[21] R. M. Wentzcovitch, W. W. Schulz, and P. B. Allen, Phys. Rev. Lett. **72**, 3389 (1994).

[22] H.-T. Kim, Y. W. Lee, B.-J. Kim, B.-G. Chae, S. J. Yun, K.-Y. Kang, K.-J. Han, K.-J. Yee, and Y.-S. Lim, Phys. Rev. Lett. **97**, 266401 (2006).

[23] A. Furube, L. Du, K. Hara, R. Katoh, and M. Tachiya, J. Am. Chem. Soc. **129**, 14852 (2007).

[24] G. Stefanovich, A. Pergament, and D. Stefanovich, J. Phys.: Condens. Matter **12**, 8837 (2000).

[25] G. Xu, C.-M. Huang, M. Tazawa, P. Jin, D.-M. Chen, and L. Miao, Appl. Phys. Lett. **93**, 061911 (2008).

[26] D. W. Ferrara, E. R. MacQuarrie, J. Nag, A. B. Kaye, R. F. Haglund, Jr., Appl. Phys. Lett. **98**, 241112 (2011).

[27] K. Appavoo, N. F. Brady, M. Seo, J. Nag, R. P. Prasankumar, D. J. Hilton, R. F. Haglund, Jr., in *CLEO: QELS – Fundamental Science*, OSA Technical Digest (Optical Society of America, Washington, 2012), paper QTh5B.5.

[28]S. D. Brorson, J. G. Fujimoto, and E. P. Ippen, Phys. Rev. Lett. **59**, 1962 (1987).
[29]J. Hohlfeld, S.-S. Wellershoff, J. Guedde, U. Conrad, V. Jaehnke, and E. Matthias, Chem. Phys. **251**, 237 (2000).
[30]G. Moriena, M. Hada, G. Sciaini, J. Matsuo, and R. J. D. Miller, J. Appl. Phys. **111**, 043504 (2012).
[31]D. Maurer, A. Leue, R. Heichele, and V. Muller, Phys. Rev. B **60**, 13249 (1999).
[32]Z. Lin, L. V. Zhigilei, and V. Celli, Phys. Rev. B **77**, 075133 (2008).
[33]G. Sciaini and R. J. D. Miller, Rep. Prog. Phys. **74**, 096101 (2011).